Journal of Alloys and Compounds 866 (2021) 158969

Contents lists available at ScienceDirect

Journal of Alloys and Compounds

journal homepage: www.elsevier.com/locate/jalcom

Zinc ions doped cesium lead bromide perovskite nanocrystals with enhanced efficiency and stability for white light-emitting diodes

Renjie Chen[a], Yan Xu[a], Song Wang[a], Chao Xia[a], Yunpeng Liu[a], Bingjie Yu[a], Tongtong Xuan[b,c,*], Huili Li[a,**]

[a] Engineering Research Center for Nanophotonics and Advanced Instrument, Ministry of Education, School of Physics and Electronic Science, East China Normal University, Shanghai 200062, China
[b] College of Materials, Xiamen University, Xiamen 361005, China
[c] Shenzhen Research Institute of Xiamen University, Shenzhen 518000, China

ARTICLE INFO

Article history:
Received 6 November 2020
Received in revised form 9 January 2021
Accepted 26 January 2021
Available online 30 January 2021

Keywords:
Cesium lead halide perovskite
Nanocrystals
PLQY
WLED

ABSTRACT

All-inorganic cesium lead halide perovskite nanocrystals (NCs) are considered as an excellent candidate material for light-emitting devices (LED) displays because of their great photo-physical properties. However, the efficiency and stability of these materials are still unsatisfactory, which is the main disadvantage hindering the commercialization of the perovskite NCs based LED displays. On the other hand, the poisonous element lead (Pb) restricted the large-scale application of the perovskite NCs. Here we reported a hot-injection method by doping zinc ions into the CsPbBr3 NCs with enhanced photoluminescence (PL) properties and stability in ambient air. The doped NCs exhibit the highest photoluminescence quantum yield (PLQY) of 91.3% and a narrow full width at half-maximum (FWHM) of 15.5 nm. The improved the optical properties and stability of the doped NCs may result from the enhanced formation energies of perovskite lattices and the surface passivation. Finally, a white light-emitting diode (WLED) was fabricated by combining the green-emitting $CsPbBr_3$:Zn^{2+} doped NCs and red-emitting K_2SiF_6:Mn^{6+} phosphors along with a blue LED chip, which exhibits a luminous efficiency of 36 lm/W, a chromaticity coordinate of (0.327, 0.336), a color temperature (CCT) of 5760 K and a wide color gamut (137% of the National Television System Committee).

1. Introduction

Inorganic lead halide perovskite nanocrystals (NCs) have attracted many researchers' attention due to their outstanding physicochemical properties , such as high photoluminescence quantum yield (PLQY), wide tunable emission wavelength, high defect tolerance, etc. Thus, the perovskite NCs have great potential applications in solar cells, Light Emitting Diodes (LEDs), and photo-electric detector [1–8]. However, the perovskite NCs suffer from poor stability because of moisture, oxygen and heat, and toxicity of lead ions, which limits their practical applications [6,7,9,10].

Many efforts have been made to improve the stability and reduce the toxicity of the lead halide perovskite NCs, which can be divided into two strategies [6,11–14]. On the one hand, to improve water stability of the NCs through coating or encapsulation of waterproof organic ligands, polymers, and silica [12,15–18]. For example, Li et al. and Konidakis et al. encapsulated the perovskite NCs in silica and $AgPO_3$ with improved hydrolytic resistance [19,44]. Zhong et al. reported that the encapsulation of the NCs in polymers with bright emission and enhanced water stability [20,21]. In our previous work, the perovskite NCs were coated with alkyl phosphate, which not only retain excellent optical properties but also exhibit high stability against water [22]. However, the thermodynamic stability of the perovskite NCs is still poor, which hinders their practical applications. On the other hand, improving the stability of the perovskite NCs by doping metal ions into perovskite structure due to the enhancing the formation energy. For instance, Mn^{2+} ions were doped into the $CsPbX_3$ (X = Cl, Br, I) NCs with improved thermal stability and excellent optical properties [23–26]. Moreover, the addition of K^+, Ni^{2+} Ce^{3+} can improve PLQY by modifying the lattice quality and reducing the trap defects [24,26–28]. Therefore, doping metal ions into the perovskite structure is an effective strategy to enhance the comprehensive stability (water, heat, oxygen, and light) and optical properties of the perovskite NCs.

* Corresponding author at: College of Materials, Xiamen University, Xiamen 361005, China.
** Corresponding author.
E-mail addresses: ttxuan@xmu.edu.cn (T. Xuan), hlli@phy.ecnu.edu.cn (H. Li).

https://doi.org/10.1016/j.jallcom.2021.158969
0925-8388/

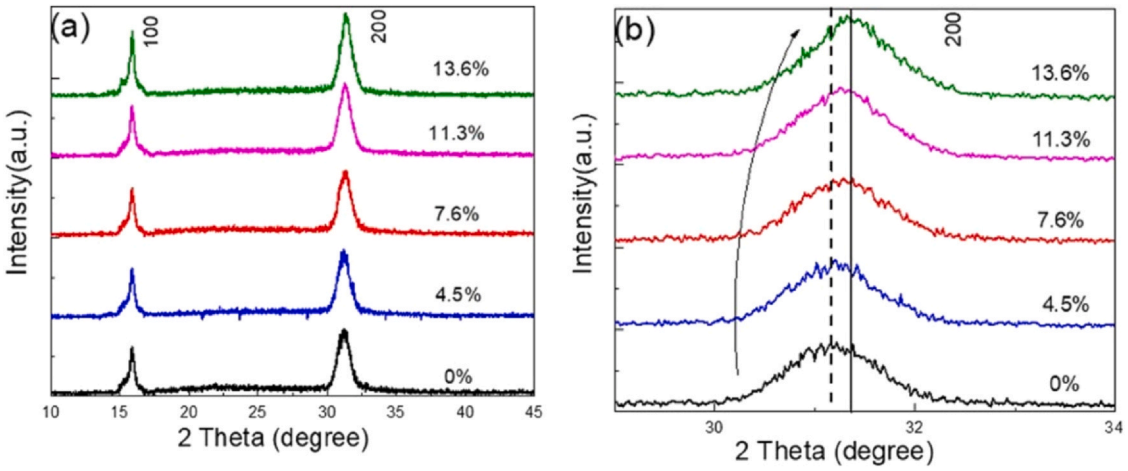

Fig. 1. XRD patterns. (a) X-ray diffraction spectra patterns of perovskite NCS with a series concentration addition of Zn^{2+} ion, (b) zoomed picture of the (200) peak.

Zinc ions show low toxicity and smaller ionic radius (74 pm) than that of Pb^{2+}(119 pm) [29,30]. Simultaneously, previous reports proved that the introduction of Zn-I could effectively passivate the surface and inside defects of organic-inorganic hybrid perovskite films and $CsPbBr_3$, $CsPbI_3$ NCs [29,30]. During the experiment and preparing of this work, we also notice the paper in JACS [38]. In the paper, the author produced the zinc addition perovskite NCs by post treatment method that adding zinc bromide salt into the synthesized original CsPbBr3 perovskite NCs toluene solution and there is no obvious change in the size of NCs. Thus, the blue shift can be attributed to the doping of Zn^{2+} ions. However, in our work, we prepared the perovskite NCs by hot injection method (Supporting Information), substituting different concentration of $PbBr_2$ by adding $ZnBr_2$ salt in the precursor solution, which can influence the crystallization process and size of the NCs. The bigger perovskite NCs size have gotten, therefore the red shift of PL emission peak has been observed in our work. Furthermore, we proposed to enhance the efficiency and stability of $CsPbBr_3$ NCs through doping Zn^{2+} ions into the perovskite NCs. The doped NCs exhibit excellent optical properties and enhanced thermal and ambient stability with the highest PLQY of 91.3% and a narrow full width at half maximum (FWHM) of 15.5 nm. Therefore, a white light-emitting diode (WLED) was fabricated by combining the green-emitting $CsPbBr_3$:Zn^{2+} NCs and red-emitting K_2SiF_6:Mn^{4+} (KSF) phosphors with a blue LED chip. The WLED shows high luminous efficiency and wide color gamut. These indicate that the doped NCs have potential application for liquid crystal display (LCD) backlight devices.

2. Results and discussion

For further exploring the effect of the introduction of Zn^{2+} ions on the chemical structure, morphology, luminescence properties and stability of doped $CsPbBr_3$ NCs, a series of NCs were prepared by a traditional hot injection method [31,32], which added different ratio concentration molar of $ZnBr_2$ compare to $PbBr_2$(from 0%, 10%, 20%, 30%, 40%) into the original precursor [32]. The actual content of zinc ion in these series NCs crystal have been detected by XPS and EDX system, which are 0%, 4.5% 7.6%, 11.3%, 13.6% respectively to each addition concentration. The X-ray diffraction (XRD) patterns of the NCs with different Zn^{2+} doping concentration are shown in Fig. 1a. It can be clearly noticed that the introduction of Zn^{2+} ions does not significantly change the chemical structure or produce Impurities into the system. The enlarged diffraction peaks of (200) lattice planes are exhibited in the Fig. 2b, it is obvious that the diffraction peaks gradually shift to higher degree as the increasing of Zn^{2+} doping concentration, which indicates the shrinkage of the perovskite lattices. It can be explained that the radius of Zn^{2+} (74 pm) is smaller than that of the Pb^{2+} (119 pm) [29]. According to this result and the previous works [29,31,32], it is convinced that zinc ion has been doped into perovskite lattice. At same time, the FWHM of the corresponding (200) peaks gradually becomes narrower along with the increasing of Zn^{2+} concentration (Table S1, S2), the shift trend of (100) peaks is matched with the (200) peak. According to the Scherrer equation, it is found that the calculated grain size of these series NCs gradually increases from 8.04 nm to 8.33 nm [33].

To further investigate the influence of Zn^{2+} ions doping on the micro-morphology of the perovskite NCs, the transmission electron microscopy (TEM) and high-resolution TEM (HR-TEM) of the NCs were carried out , as shown in Fig. 2. All the perovskite NCs show uniform cubic crystals. Meanwhile, with the increasing of the Zn^{2+} doping concentration, the average size of the NCs was increased from 9.6 ± 2.1 nm to 10.1 ± 1.9 nm, 11.3 ± 2.3 nm, 12.6 ± 1.7 nm and 12.8 ± 1.5 nm, which are shown in the Fig. 2(f) and S2. From the HR-TEM images at the right upper of each figure, the lattice space *d* of (100) decreases from 0.60 nm to 0.59 nm. These results agree well with the analysis of XRD patterns data (Fig. 1), which further proves that zinc ions were doped into the perovskite lattices. The effect that zinc ion doping on the morphology of the perovskite NCs is mainly focus on the adjustment of grain size. It may result from that zinc ions have a higher charge attraction than that of Pb^{2+} ions, and it is easier to attract and be attracted by surrounding bromine ions during the formation of perovskite NCs [34,35]. Furthermore, from the EDS mapping patterns in Fig. S1, zinc ions are evenly distributed in the perovskite NCs. Combining the results of XRD patterns and TEM images, it is safely determined that Zn ions have been successfully doped into $CsPbBr_3$ perovskite lattices. The mechanism that zinc ion effect on the morphology could be summarized as in Fig. 3c.

To evaluate the Zn^{2+} ions concentration in the NCs, we further employed the X-ray photoelectron spectroscopy (XPS) to detect the NCs ions interaction before and after the addition of Zn ions. In Fig. 4a and b, it shows obvious XPS signal peak of C 2s, N 2p, Pb 4f, Br 2p, Cs 3d. The binding energy of Zn $2p_{1/2}$ and Zn $2p_{3/2}$ for $CsPbBr_3$:Zn^{2+} doped NCs is located at 1045.6 eV and 1022.3 eV,

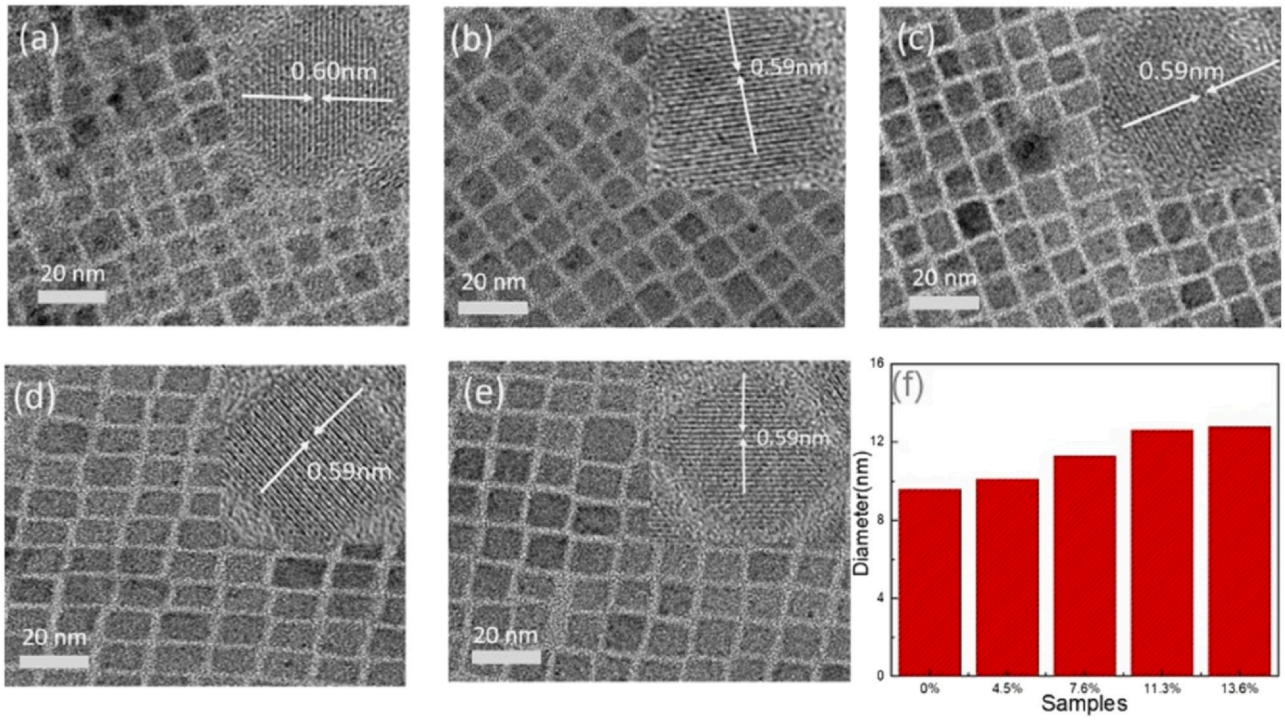

Fig. 2. (a–e) TEM images of $CsPbBr_3$ PNCs with different ration of $ZnBr_2$.(a) 0%,(b) 4.5%, (c) 7.6%, (d) 11.3%, (e) 11.6%; upper right are the HRTEM patterns. (f) the average grain size Histogram of the series NCs.

respectively, which matches well with the 2p singles of Zn^{2+} in perovskite NCs [29,36,37]. The signal of Pb $4f_{7/2}$ moves from 138.6 eV in the original NCs to the lower binding energy axis of 138.5 eV in the doped NCs [10,30]. Meanwhile, the Br 3d orbit of different samples exhibit similar binding energy (68.3 eV). After the split and fit of the Br XPS peak (Fig. S5). The peak location of Br $3d_{3/2}$ and $3d_{5/2}$ are located at the 68.3 eV, 69.4 eV, which indicates the existence of Br element in perovskite NCs [26,45], and the other Br $3d_{5/2}$ at the peak of 66.4 eV is attribute the existence of Br-Br bond on the NCs surface [46,47]. There are have no obvious peak location change of Br element in the original and doped NCs sample. This result indicates the binding energy between Pb with Br is weakened after the introduction of Zn^{2+} ions. By deeply considering, in the doped NCs, the higher chemical activity element Zn^{2+} ions are partly substituting the location of Pb^{2+} ions and interacting with Br ions, which weakens the binding energy between Pb and Br due to the higher chemical attraction [29,37,47]. Table S3 shows the molar ratio of Zn^{2+} to Pb^{2+} by using XPS and EDX systems, which illustrates that the actual Zn^{2+} concentrations of the 0%, 10%, 20%, 30%, 40% doping perovskite NCs samples are about 0%, 4.5%, 7.6%, 11.3%, 13.6%, respectively.

Furthermore, the PL properties of the perovskite NCs has been investigated in detail. The steady-state PL spectra of pristine and doped NCs with different Zn^{2+} doping concentration were shown in Fig. 4a. As the increasing of the Zn^{2+} ions doping concentration from 0% to 13.6%, the PL peaks were shifted from 509.1 nm to 515.5 nm. The absorbance edge show the uniform red shift trend after the addition of zinc ion, which is matched with the PL emission peaks (Fig. S3) According to previous paper, the zinc salts usually have a large band gap, zinc ions contribute negligible effect to the in-gap trap energy alignment of perovskite structure, so we summarize the phenomenon to the increased size and quantum size effect of the NCs (Fig. 3) [29,36,38]. The PLQY of the perovskite NCs (Table 1) does not continuously enhances with increase of Zn^{2+} doping concentration but presents an optimal passivation value at 11.3%, which exhibits the highest PLQY of 91.3%, and the narrowest FWHM of 15.5 nm. The PLQY data of the original and 11.3% zinc doped sample has been shown in the Fig. S6. As the Zn^{2+} doping concentration rising to 13.6%, the excess introduction of Zinc structure perovskite substitute the intrinsic luminescent center of $CsPbBr_3$ perovskite crystal, therefore the over-doped NCs owns more recombination center and shows the low PLQY value of 76.5% [29]. As we know, the narrower PL emission peak means higher color purity, which has great advantage in the field of high-quality lighting and displays. It can be attributed to the surface defect passivation and increased formation energy [39,40]. For the further study the PL mechanism of the perovskites NCs, we employed the transient PL spectroscopy to detect the recombination process in the perovskite NCs (Fig. 3b). The time-resolved PL decay curves fitted by the bi-exponential equation [29,41].

$$I(t) = A_1 e^{(\frac{-t}{\tau_1})} + A_2 e^{(\frac{-t}{\tau_2})}$$

where A_1 and A_2 are the relative amplitudes, τ_1 and τ_2 represent the lifetimes of the two recombination ways (fast and slow). The fast decay process is attributed to the exciton recombination from the conductive band to valence band, and the slow decay represents trap-assisted recombination in its bulk or surface [8,14,42]. The NCs with the addition of Zn^{2+} ion exhibits fast and slow lifetimes of 1.92 ns ($A_1 = 0.15$) and $\tau_2 = 71.6$ ns ($A_2 = 0.85$) and the average photocarrier life time of 46,8 ns, respectively. In contrast, the pristine NCs show $\tau_1 = 2.15$ ns ($A_1 = 0.24$) and $\tau_2 = 57.6$ ns ($A_2 = 0.76$) and average

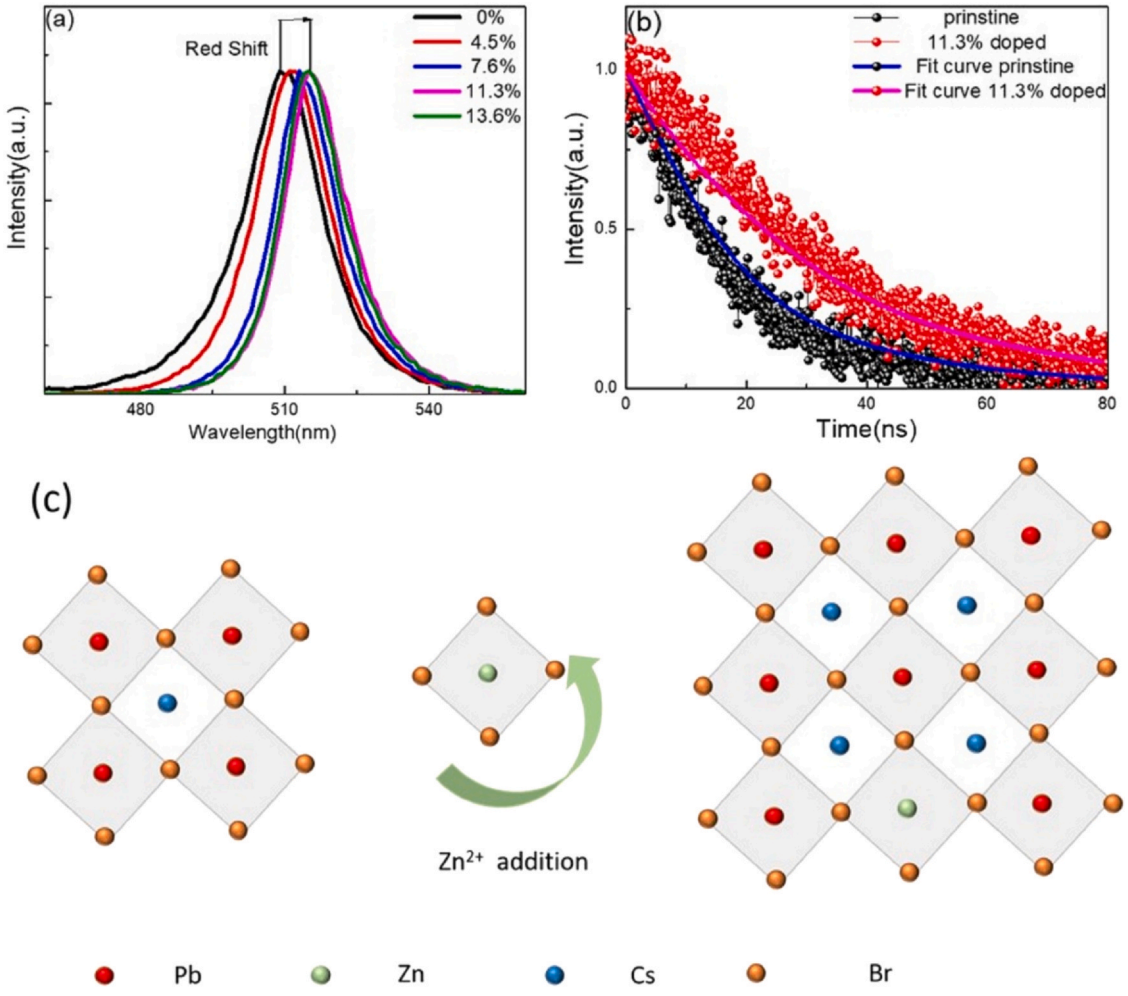

Fig. 3. (a) The steady-state PL spectra, (b) the Time resolved PL decay curves, (c) the mechanism that Zn ion act on perovskite NCs.

time of 43.1 ns. The longer τ_2 means lower recombination rate of photo-carrier from conductive band to defects in doped NCs, which means there has lesser trap defects in the doped perovskite QDs. Therefore, this result reveals that the enhanced efficiency of doped NCs is relate to the reduced defects correspond well with the analysis of the PLQY [29].

Furthermore, we evaluated the thermal and air ambient stability of pristine and 11.3% Zn^{2+} doped $CsPbBr_3$ perovskite NCs by heating them from 300 K to 420 K and then cooling down to room temperature. As shown in Fig. 5a, the relative PL intensity of the doped NCs maintained 40% of initial value at 350 K, which is higher than the pristine $CsPbBr_3$ NCs (26.8%). After the heating-cooling circulation process, the doped NCs maintained 41.1% of the original PL intensity, while the pristine NCs reversed only 26.1%. These results indicate that the Zn^{2+} ions doped $CsPbBr_3$ NCs exhibit enhanced thermal stability. The ambient stability (Fig. 5b) of pristine and doped NCs were studied by keeping the NCs for 168 h under ambient conditions (at the temperature of 295 K and 30–40% RH). It is obvious that after aging 168 h, the doped NCs maintained 92.1% of original value, which is higher than the pristine NCs (76.3%). According to previous works, the doping of metal ions like Mn, Zn, Cd into perovskite NCs can improve its thermal and ambient stability due to enhanced formation energy, which was proved by DFT calculation in their paper [23,25,43]. Meanwhile, the better crystal quality is also benefit to the NCs stability [28]. The stability is verified by the UV–vis absorbance test (Fig. S4), the optimal doped sample shows the lesser absorbance drop after aged for 168 h in ambient condition. Therefore, we attribute the increased thermal stability and ambient stability to the increase of formation energy and better crystal quality after the doping of zinc ions.

Finally, a white light-emitting diode (WLED) was fabricated by combining the green-emitting Zn doped $CsPbBr_3$ perovskite NCs and red-emitting $K_2SiF_6:Mn^{6+}$ (KSF) phosphors with a blue-emitting LED chip. The device shows bright white emission (Fig. 6) with a color coordinates of (0.327, 0.336) and a correlated color temperature (CCT) of 5760 K. Furthermore, the WLED exhibits a luminous efficiency of 36 lm/W and wide color gamut (137% of National Television System Committee, NTSC). Thus, the zinc doped NCs have great potential in high quality displays.

3. Conclusion

In summary, we presented Zn^{2+} ions doped $CsPbBr_3$ NCs with enhanced optical properties. The optimized doped NCs exhibit the highest

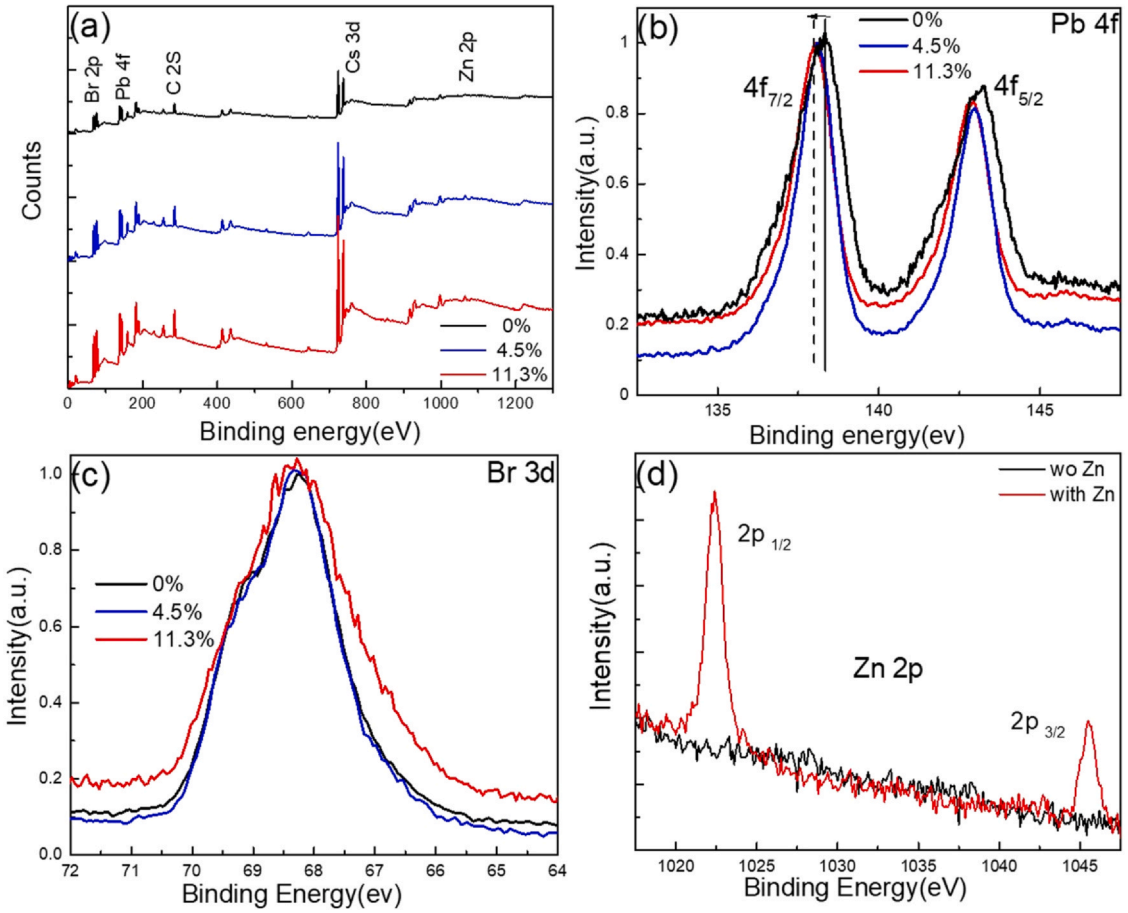

Fig. 4. XPS core spectra. (a) Full spectra of these samples (b) Pb 4f, (c) Br 3d, (d) Zn 2p.

Table 1
PL properties of the undoped and doped perovskite NCs.

Sample	Peak location (nm)	FWHM (nm)	PLQY (%)
0%	509.1	19.0	78.4 ± 3.14
4.5%	511.2	17.9	81.3 ± 3.24
7.6%	512.9	15.5	85.1 ± 3.56
11.3%	514.4	15.5	91.3 ± 3.82
13.6%	514.6	15.6	76.5 ± 3.07

PLQY of 91.3% and a FWHM of 15.5 nm. Furthermore, the $CsPbBr_3$:Zn^{2+} NCs show enhanced thermal and air ambient stability. Finally, a WLED was fabricated based on green-emitting $CsPbBr_3$:Zn^{2+} NCs, red-emitting KSF phosphors, and a blue LED chip. The device shows a wide color gamut (137% of NTSC) and a luminous efficiency of 36 lm/W. We believe that the employment of doping Zn^{2+} ions into perovskites to improve the stability and optical properties will energetically facilitate their application in LED displays.

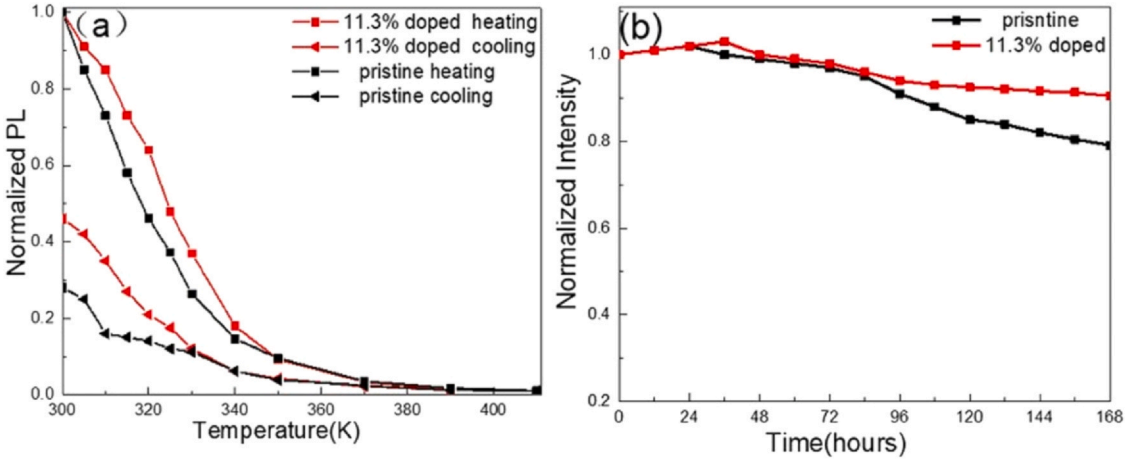

Fig. 5. Stability properties. (a) thermal stability, (b) air ambient stability.

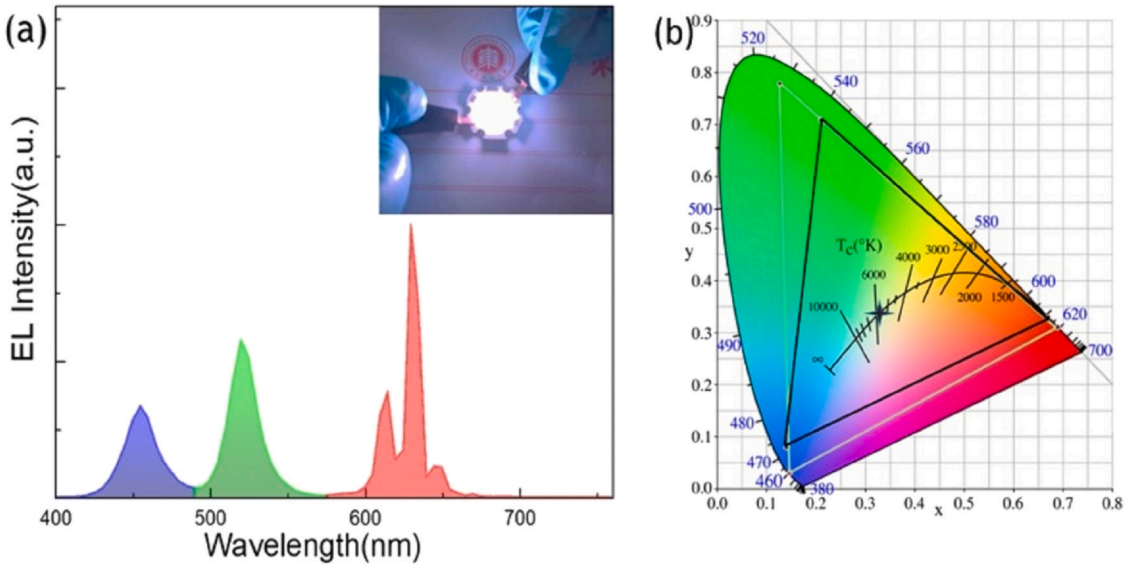

Fig. 6. (a) The EL spectrum of based on Zn doped $CsPbBr_3$ NCs, KSF phosphors and a blue LED chip. The inset photograph shows the WLED under working condition. (b) The color coordinate and the color gamut of as-fabricated WLED.

CRediT authorship contribution statement

Renjie Chen: the main task preparing NCs materials, test and writing. **Yan Xu:** Assist preparing NCs, PL, PLQY test. **Song Wang:** Assist WLED test. **Chao Xia:** TRPL test. **Yunpeng Liu:** Assist PL test. **Bingjie Yu:** Assist WLED test. **Tongtong Xuan:** Writing - reviewing & editing. **Huili Li:** Writing - reviewing & editing.

Declaration of Competing Interest

The authors declare that they have no known competing financial interests or personal relationships that could have appeared to influence the work reported in this paper.

Acknowledgements

This work is supported by Shanghai Municipal Natural Science Foundation (No. 19ZR1415400), East China Normal University-University of Alberta Joint Institute of Advanced Science and Technology (JIAST) (No. 40500-20105-222053), the National Natural Science Foundation of China (No. 51702373, No. 51472087), the Natural Science Foundation of Fujian Province (No. 2020J01035), the "Double-First Class" Foundation of Materials and Intelligent Manufacturing Discipline of Xiamen University and the Fundamental Research Funds for the Central Universities (No. 2072020078).

Appendix A. Supporting information

Supplementary data associated with this article can be found in the online version at doi:10.1016/j.jallcom.2021.158969.

References

[1] J. Dai, J. Xi, L. Li, J. Zhao, Y. Shi, W. Zhang, C. Ran, B. Jiao, X. Hou, X. Duan, Z. Wu, Charge transport between coupling colloidal perovskite quantum dots assisted by functional conjugated ligands, Angew. Chem. 57 (2018) 5754–5758, https://doi.org/10.1002/anie.201801780
[2] T. Matsushima, S. Hwang, A.S. Sandanayaka, C. Qin, S. Terakawa, T. Fujihara, M. Yahiro, C. Adachi, Solution-processed organic-inorganic perovskite field-effect transistors with high hole mobilities, Adv. Mater. 28 (2016) 10275–10281, https://doi.org/10.1002/adma.201603126
[3] M.A. Green, A. Ho-Baillie, H.J. Snaith, The emergence of perovskite solar cells, Nat. Photonics 8 (2014) 506–514, https://doi.org/10.1038/nphoton.2014.134
[4] H. Zhou, Q. Chen, G. Li, S. Luo, T.B. Song, H.S. Duan, Z. Hong, J. You, Y. Liu, Y. Yang, Photovoltaics. Interface engineering of highly efficient perovskite solar cells, Science 345 (2014) 542–546, https://doi.org/10.1126/science.1254050
[5] M. Liu, M.B. Johnston, H.J. Snaith, Efficient planar heterojunction perovskite solar cells by vapour deposition, Nature 501 (2013) 395–398, https://doi.org/10.1038/nature12509
[6] B. Han, B. Cai, Q. Shan, J. Song, J. Li, F. Zhang, J. Chen, T. Fang, Q. Ji, X. Xu, H. Zeng, Stable, efficient red perovskite light-emitting diodes by (α, δ)-CsPbI3 phase engineering, Adv. Funct. Mater. 28 (2018) 1804285, https://doi.org/10.1002/adfm.201804285
[7] X. Ling, S. Zhou, J. Yuan, J. Shi, Y. Qian, B.W. Larson, Q. Zhao, C. Qin, F. Li, G. Shi, C. Stewart, J. Hu, X. Zhang, J.M. Luther, S. Duhm, W. Ma, 14.1% CsPbI3 perovskite quantum dot solar cells via cesium cation passivation, Adv. Energy Mater. 9 (2019) 1900721, https://doi.org/10.1002/aenm.201900721
[8] D. Shi, V. Adinolfi, R. Comin, M. Yuan, E. Alarousu, A. Buin, Y. Chen, S. Hoogland, A. Rothenberger, K. Katsiev, Low trap-state density and long carrier diffusion in organolead trihalide perovskite single crystals, Science 347 (2015) 519–522, https://doi.org/10.1038/s41586-018-0575-3
[9] F. Liu, Y. Zhang, C. Ding, S. Kobayashi, T. Izuishi, N. Nakazawa, T. Toyoda, T. Ohta, S. Hayase, T. Minemoto, K. Yoshino, S. Dai, Q. Shen, Highly luminescent phase-stable CsPbI3 perovskite quantum dots achieving near 100% absolute photoluminescence quantum yield, ACS Nano 11 (2017) 10373–10383, https://doi.org/10.1021/acsnano.7b05442
[10] D. Bi, C. Yi, J. Luo, J.-D. Décoppet, F. Zhang, Shaik M. Zakeeruddin, X. Li, A. Hagfeldt, M. Grätzel, Polymer-templated nucleation and crystal growth of perovskite films for solar cells with efficiency greater than 21%, Nat. Energy 1 (2016) 1–5, https://doi.org/10.1038/nenergy.2016.142
[11] T. Xuan, J. Huang, H. Liu, S. Lou, L. Cao, W. Gan, R.-S. Liu, J. Wang, Super-hydrophobic cesium lead halide perovskite quantum dot-polymer composites with high stability and luminescent efficiency for wide color gamut white light-emitting diodes, Chem. Mater. 31 (2019) 1042–1047, https://doi.org/10.1021/acs.chemmater.8b04596
[12] D. Yan, T. Shi, Z. Zang, T. Zhou, Z. Liu, Z. Zhang, J. Du, Y. Leng, X. Tang, Ultrastable CsPbBr3 perovskite quantum dot and their enhanced amplified spontaneous emission by surface ligand modification, Small 15 (2019) e1900606, https://doi.org/10.1002/smll.201901173
[13] R. An, F. Zhang, X. Zou, Y. Tang, M. Liang, I. Oshchapovskyy, Y. Liu, A. Honarfar, Y. Zhong, C. Li, H. Geng, J. Chen, S.E. Canton, T. Pullerits, K. Zheng, Photostability and photodegradation processes in colloidal $CsPbI_3$ perovskite quantum dots, ACS Appl. Mater. Interfaces 10 (2018) 39222–39227, https://doi.org/10.1021/acsami.8b14480
[14] Z. Li, L. Kong, S. Huang, L. Li, Highly luminescent and ultrastable CsPbBr3 perovskite quantum dots incorporated into a silica/alumina monolith, Angew. Chem. 129 (2017) 8246–8250, https://doi.org/10.1021/acsenergylett.9b00209
[15] X.G. Wu, J. Tang, F. Jiang, X. Zhu, Y. Zhang, D. Han, L. Wang, H. Zhong, Highly luminescent red emissive perovskite quantum dots-embedded composite films: ligands capping and caesium doping-controlled crystallization process, Nanoscale 11 (2019) 13697–13707, https://doi.org/10.1039/c8nr10036e
[16] J. Zhang, Y. Huang, X. Jin, A. Nazartchouk, M. Liu, X. Tong, Y. Jiang, L. Ni, S. Sun, Y. Sang, H. Liu, L. Razzari, F. Vetrone, J. Claverie, Plasmon enhanced upconverting core@triple-shell nanoparticles as recyclable panchromatic initiators (blue to infrared) for radical polymerization, Nanoscale Horiz. 4 (2019) 907–917, https://doi.org/10.1039/c9nh00026g

[17] A. Dutta, S.K. Dutta, S. Das Adhikari, N. Pradhan, Tuning the size of $CsPbBr_3$ nanocrystals: all at one constant temperature, ACS Energy Lett. 3 (2018) 329–334, https://doi.org/10.1021/acsenergylett.7b01226
[18] S. Zou, C. Liu, R. Li, F. Jiang, X. Chen, Y. Liu, M. Hong, From nonluminescent to blue-emitting Cs_4PbBr_6 nanocrystals: tailoring the insulator bandgap of 0D perovskite through Sn cation doping, Adv. Mater. 31 (2019) 1900606, https://doi.org/10.1002/adma.201900606
[19] S. Huang, Z. Li, L. Kong, N. Zhu, A. Shan, L. Li, Enhancing the stability of $CH_3NH_3PbBr_3$ quantum dots by embedding in silica spheres derived from tetramethyl orthosilicate in "waterless" toluene, J. Am. Chem. Soc. 138 (2016) 18044–18052, https://doi.org/10.1021/jacs.5b13101
[20] Q. Zhou, Z. Bai, W.G. Lu, Y. Wang, B. Zou, H. Zhong, In situ fabrication of halide perovskite nanocrystal-embedded polymer composite films with enhanced photoluminescence for display backlights, Adv. Mater. 28 (2016) 9163–9168, https://doi.org/10.1002/adma.201602651
[21] H. Kim, S. So, A. Ribbe, Y. Liu, W. Hu, V.V. Duzhko, R.C. Hayward, T. Emrick, Functional polymers for growth and stabilization of $CsPbBr_3$ perovskite nanoparticles, Chem. Commun. 55 (2019) 1833–1836, https://doi.org/10.1039/c8cc09343a
[22] T. Xuan, X. Yang, S. Lou, J. Huang, Y. Liu, J. Yu, H. Li, K.-L. Wong, C. Wang, J. Wang, Highly stable $CsPbBr_3$ quantum dots coated with alkyl phosphate for white light-emitting diodes, Nanoscale 9 (2017) 15286–15290, https://doi.org/10.1039/C7NR04179A
[23] S. Zou, Y. Liu, J. Li, C. Liu, R. Feng, F. Jiang, Y. Li, J. Song, H. Zeng, M. Hong, X. Chen, Stabilizing cesium lead halide perovskite lattice through Mn(II) substitution for air-stable light-emitting diodes, J. Am. Chem. Soc. 139 (2017) 11443–11450, https://doi.org/10.1021/jacs.7b04000
[24] J.S. Yao, J. Ge, B.N. Han, K.H. Wang, H.B. Yao, H.L. Yu, J.H. Li, B.S. Zhu, J.Z. Song, C. Chen, Q. Zhang, H.B. Zeng, Y. Luo, S.H. Yu, Ce(3+)-doping to modulate photoluminescence kinetics for efficient $CsPbBr_3$ nanocrystals based light-emitting diodes, J. Am. Chem. Soc. 140 (2018) 3626–3634, https://doi.org/10.1021/jacs.7b11955
[25] J. Yin, G.H. Ahmed, O.M. Bakr, J.-L. Brédas, O.F. Mohammed, Unlocking the effect of trivalent metal doping in all-inorganic $CsPbBr_3$ perovskite, ACS Energy Lett. 4 (2019) 789–795, https://doi.org/10.1021/acsenergylett.9b00209
[26] S. Thawarkar, P.J.S. Rana, R. Narayan, S.P. Singh, Ni-doped CsPbBr3 perovskite: synthesis of highly stable nanocubes, Langmuir 35 (2019) 17150–17155, https://doi.org/10.1021/acs.langmuir.9b02450
[27] S. Huang, B. Wang, Q. Zhang, Z. Li, A. Shan, L. Li, Postsynthesis potassium-modification method to improve stability of $CsPbBr_3$ perovskite nanocrystals, Adv. Opt. Mater. 6 (2018) 1701106, https://doi.org/10.1002/adom.201701106
[28] Y. Hu, F. Bai, X. Liu, Q. Ji, X. Miao, T. Qiu, S. Zhang, Bismuth incorporation stabilized α-CsPbI3 for fully inorganic perovskite solar cells, ACS Energy Lett. 2 (2017) 2219–2227, https://doi.org/10.1021/acsenergylett.7b00508
[29] X. Shen, Y. Zhang, S.V. Kershaw, T. Li, C. Wang, X. Zhang, W. Wang, D. Li, Y. Wang, M. Lu, L. Zhang, C. Sun, D. Zhao, G. Qin, X. Bai, W.W. Yu, A.L. Rogach, Zn-alloyed $CsPbI_3$ nanocrystals for highly efficient perovskite light-emitting devices, Nano Lett. 19 (2019) 1552–1559, https://doi.org/10.1021/acs.nanolett.8b04339
[30] H. Sun, J. Zhang, X. Gan, L. Yu, H. Yuan, M. Shang, C. Lu, D. Hou, Z. Hu, Y. Zhu, L. Han, Pb-reduced $CsPb_{0.9}Zn_{0.1}I_2Br$ thin films for efficient perovskite solar cells, Adv. Energy Mater. 9 (2019) 1900896, https://doi.org/10.1002/aenm.201900896
[31] X. Li, Y. Wu, S. Zhang, B. Cai, Y. Gu, J. Song, H. Zeng, CsPbX3 quantum dots for lighting and displays: room-temperature synthesis, photoluminescence superiorities, underlying origins and white light-emitting diodes, Adv. Funct. Mater. 26 (2016) 2435–2445, https://doi.org/10.1002/adfm.201600109
[32] J. Song, J. Li, X. Li, L. Xu, Y. Dong, H. Zeng, Quantum dot light-emitting diodes based on inorganic perovskite cesium lead halides ($CsPbX_3$), Adv. Mater. 27 (2015) 7162–7175, https://doi.org/10.1002/adma.201502567
[33] U. Holzwarth, N. Gibson, The Scherrer equation versus the 'Debye-Scherrer equation', Nat. Nanotechnol. 6 (2011) 534, https://doi.org/10.1038/nnano.2011.145
[34] G.J. Hutchings, Vapor phase hydrochlorination of acetylene: correlation of catalytic activity of supported metal chloride catalysts, J. Catal. 96 (1985) 292–295, https://doi.org/10.1016/0021-9517 (85) 90383-5
[35] T. Dudev, C. Lim, Metal binding and selectivity in Zinc proteins, J. Chin. Chem. Soc. 50 (2003) 1093–1102, https://doi.org/10.1002/jccs.200300155
[36] P. Tyagi, A.G. Vedeshwar, Optical properties of ZnI2 films, Phys. Rev. B 64 (2001) 245406, https://doi.org/10.1103/PhysRevB.64.245406
[37] R. Chen, D. Hou, C. Lu, J. Zhang, P. Liu, H. Tian, Z. Zeng, Q. Xiong, Z. Hu, Y. Zhu, L. Han, Zinc ion as effective film morphology controller in perovskite solar cells, Sustain. Energ. Fuels 2 (2018) 1093–1100, https://doi.org/10.1039/c8se00059j
[38] W. van der Stam, J.J. Geuchies, T. Altantzis, K.H. van den Bos, J.D. Meeldijk, S. Van Aert, S. Bals, D. Vanmaekelbergh, C. de Mello Donega, Highly emissive divalent-ion-doped colloidal $CsPb_{1-x}M_xBr_3$ perovskite nanocrystals through cation exchange, J. Am. Chem. Soc. 139 (2017) 4087–4097, https://doi.org/10.1021/jacs.6b13079
[39] Z. Yang, M. Wei, O. Voznyy, P. Todorovic, M. Liu, R. Quintero-Bermudez, P. Chen, J.Z. Fan, A.H. Proppe, L.N. Quan, G. Walters, H. Tan, J.W. Chang, U.S. Jeng, S.O. Kelley, E.H. Sargent, Anchored ligands facilitate efficient B-site doping in metal halide perovskites, J. Am. Chem. Soc. 141 (2019) 8296–8305, https://doi.org/10.1021/jacs.9b02565
[40] B. Yang, X. Mao, F. Hong, W. Meng, Y. Tang, X. Xia, S. Yang, W. Deng, K. Han, Lead-free direct band gap double-perovskite nanocrystals with bright dual-color emission, J. Am. Chem. Soc. 140 (2018) 17001–17006, https://doi.org/10.1021/jacs.8b07424
[41] Q. Chen, L. Chen, F. Ye, T. Zhao, F. Tang, A. Rajagopal, Z. Jiang, S. Jiang, A.K. Jen, Y. Xie, J. Cai, L. Chen, Ag-incorporated organic-inorganic perovskite films and planar heterojunction solar cells, Nano Lett. 17 (2017) 3231–3237, https://doi.org/10.1021/acs.nanolett.7b00847
[42] X. Chen, D. Li, G. Pan, D. Zhou, W. Xu, J. Zhu, H. Wang, C. Chen, H. Song, All-inorganic perovskite quantum dot/TiO_2 inverse opal electrode platform: stable and efficient photoelectrochemical sensing of dopamine under visible irradiation, Nanoscale 10 (2018) 10505–10513, https://doi.org/10.1039/C8NR02115E
[43] S. Ye, J.Y. Sun, Y.H. Han, Y.Y. Zhou, Q.Y. Zhang, Confining $Mn^{(2+)}$-doped lead halide perovskite in zeolite-Y as ultrastable orange-red phosphor composites for white light-emitting diodes, ACS Appl. Mater. Interfaces 10 (2018) 24656–24664, https://doi.org/10.1021/acsami.8b08342
[44] I. Konidakis, K. Brintakis, A. Kostopoulou, I. Demeridou, P. Kavatzikidou, E. Stratakis, Highly luminescent and ultrastable cesium lead bromide perovskite patterns generated in phosphate glass matrices, Nanoscale 12 (2020) 13697–13707, https://doi.org/10.1039/d0nr03254a
[45] A.R. Milosavljevic, D.K. Bozanic, S. Sadhu, N. Vukmirovic, R. Dojcilovic, P. Sapkota, W. Huang, J. Bozek, C. Nicolas, L. Nahon, S. Ptasinska, Electronic properties of free-standing surfactant-capped lead halide perovskite nanocrystals isolated in Vacuo, J. Phys. Chem. Lett. 9 (2018) 3604–3611, https://doi.org/10.1021/acs.jpclett.8b01466
[46] K.H. Wang, J.N. Yang, Q.K. Ni, H.B. Yao, S.H. Yu, Metal halide perovskite supercrystals: gold-bromide complex triggered assembly of CsPbBr3 nanocubes, Langmuir 34 (2018) 595–602, https://doi.org/10.1021/acs.langmuir.7b03432
[47] J. Zhang, M.-h Shang, P. Wang, X. Huang, J. Xu, Z. Hu, Y. Zhu, L. Han, n-Type doping and energy states tuning in $CH_3NH_3Pb_{1-x}Sb_{2x/3}I_3$ perovskite solar cells, ACS Energy Lett. 1 (2016) 535–541, https://doi.org/10.1021/acsenergylett.6b00241